



## Annular Beam Driven Metamaterial Backward Wave Oscillator

Jyoti Vengurlekar\* and Ayush Saxena



Department of Electronics and Telecommunication Engineering, Ramrao Adik Institute of Technology (RAIT), D.Y. Patil Deemed to be University, Nerul, Navi Mumbai-400706, India

E-mail/Orcid Id:

JV,  [jyoti.vengurlekar@rait.ac.in](mailto:jyoti.vengurlekar@rait.ac.in),  <https://orcid.org/0000-0002-8179-2382>;

AS,  [ayush.saxena@rait.ac.in](mailto:ayush.saxena@rait.ac.in),  <https://orcid.org/0000-0001-5550-7667>

### Article History:

Received: 25<sup>th</sup> Oct., 2024

Accepted: 15<sup>th</sup> Mar., 2022

Published: 30<sup>th</sup> Mar., 2024

### Keywords:

Backward Wave Oscillator,  
Electron Beam, High power  
Microwave generation,  
Metamaterial, PIC Simulations

### How to cite this Article:

Jyoti Vengurlekar and Ayush Saxena (2024).  
Annular Beam Driven Metamaterial  
Backward Wave Oscillator. International  
Journal of Experimental Research and  
Review, 37(Spl.), 131-138.

### DOI:

<https://doi.org/10.52756/ijerr.2024.v37spl.011>

**Abstract:** Metamaterials (MTMs) are synthetic materials designed to have characteristics that "may not be readily available in nature," such as negative permittivity, reversed Doppler Effect, reversed Cherenkov Effect, and negative Refractive Index. These characteristics have motivated researchers to analyze and investigate the use of MTMs for modelling high-power microwave (HPM) radiation sources. One of the most potential HPM sources is an annular beam-driven Backward-Wave Oscillator (BWO) based on the Cerenkov mechanism. The devices that use the Cerenkov mechanism are preferred due to their larger bandwidth. Its high output power and repetition operations make it a promising source. In this paper, an annular beam-loaded metamaterial BWO is simulated in order to investigate and comment on the possibility of metamaterial or metamaterial-inspired structures replacing the slow-wave structures (SWSs) in vacuum tube devices. Performance parameters of several BWO configurations loaded with different metamaterial-inspired conductor rings are compared to rippled SWS-based BWOs. The results suggest that fewer metamaterial rings with solid cross-section (CS) inside the BWO lead to a closer match in generated output power and frequency with the output power generated using a rippled SWS.

### Introduction

Metamaterials are materials with unique electromagnetic properties not seen in nature, such as negative permeability and negative permittivity. Negative electromagnetic characteristics of MTMs enable backward wave propagation and reverse Cherenkov radiation (Tatiana et al., 2021). Recently, there has been increased interest (Jorwal et al., 2023) in researching the use of MTMs to produce HPM radiation sources. Two different types of vacuum electron devices (VEDs) have been used to create and amplify microwaves; travelling wave tubes (TWTs) and BWOs (Banerjee, 2020; Kumar et al., 2023). TWTs enhance the incoming RF signal that moves with the electron beam, whereas a BWO uses noise from the DC electron beam and the explosive emission cathode to produce a backward RF output

signal ( $v_g v_{ph} < 0$ ) (Seidfarji et al., 2019; Banerjee et al., 2014).

For generation of electromagnetic waves in VEDs, two basic requirements must be satisfied:

(1) The existence of an axial component of the electric field as required by Poynting's theorem; and (2) the phase velocity of the wave must be slightly less than the beam velocity as required by the Cherenkov resonance condition. The TWTs and BWOs are called Cherenkov devices because their electrons radiate similarly to electrons that generate Cherenkov radiation when they travel through a medium faster than the average speed of light in that medium. They are sometimes referred to as O-type devices since the electrons follow the axial DC magnetic field that guides them through the SWS interaction zone (Seidfarji et al., 2019). The



Cerenkov devices are preferred over rippled wall devices because of their larger bandwidth. The electron beam in rippled wall devices has a more limited interaction region in terms of frequency than that of a Cerenkov device (Shiffler et al., 2010).

The extensive research on MTMs over the last decades comprises exploring their extraordinary electromagnetic characteristics like negative Permittivity, negative Permeability, reversed Doppler Effect, reversed Cherenkov Effect, negative Refractive Index etc (Veselago Viktor G., 1968; Pendry et al., 1999; Smith et al., 2000; Pendry et al., 2006; Marqués et al., 2007; Simovski et al., 2009; Chen et al., 2016; Hadap et al., 2020). These exotic electromagnetic properties motivated several potential applications in the field of VEDs. Conventional VEDs, like BWOs and TWTs, work on the principle of interaction of intense electron beam with the slow wave structure to generate and amplify microwave signals (Mineo et al., 2010; Wang et al., 2013; Nguyen et al., 2014; Baig et al., 2012). For conventional VEDs, efficient interaction of beam mode with waveguide mode is always desired. Recent theoretical studies investigate the realizability of beam wave interaction in metamaterial (Tan et al., 2009; Shiffler et al., 2013; Duan et al., 2012; Shapiro et al., 2012; Duan et al., 2013; French et al., 2013) and studying the use of metamaterial for the efficiency enhancement in VEDs by beam interaction with waveguide modes and miniaturization of the conventional high-power microwave devices. The Cherenkov radiation from an electron beam moving through a SWS describes the physical mechanism in BWOs. The waveguide material (Hummelt et al., 2014) is crucial in determining the apparatus's parameters and output power. It also significantly determines the design ease and flexibility of the device. According to (Grow et al., 1955), efficiency can be increased by increasing the space-charge parameter or the gain value. It has been discovered that velocity spread, beam thickness, and circuit loss reduce efficiency.

This paper presents the analytical study of an annular beam-driven BWO using particle-in-cell (PIC) code, where a metamaterial-loaded cylindrical waveguide replaces the slow wave structure (SWS). Experimentation on HPM devices has various

limitations that can be overcome using PIC simulations (Ludeking et al., 2011; Goplen et al., 1995). High-power microwave (HPM) devices, which generate intense bursts of electromagnetic radiation in the microwave range, can be difficult to test due to several experimental limitations. These limitations can include issues with the size and complexity of the devices, the potential danger of high-power radiation, and the difficulties associated with measuring and characterizing the radiation produced. One way to overcome these limitations is to use Particle-In-Cell (PIC) simulations, which are a type of computational technique used to model the behaviour of plasmas and electromagnetic fields. PIC simulations can provide a virtual laboratory environment where researchers can test and optimize HPM devices without physical experimentation. By modelling the complex interactions between electrons, ions, and electromagnetic fields, PIC simulations can provide insights into the behaviour of HPM devices that may be difficult or impossible to obtain experimentally. The PIC simulations can be used to validate experimental data and provide a deeper understanding of the physical processes underlying experimental observations (Pan et al., 2021; Xiangyan et al., 2022). Therefore, optimizing input parameters for PIC simulations to ensure accurate and reliable results while minimizing computational cost is essential. This can involve a combination of trial and error and mathematical and computational methods to determine the optimal parameters for a given simulation.

This paper compares six different annular beam-driven BWO configurations for their peak output power, output power frequency and efficiency. These six configurations are modified versions of the BWO design presented by (Chandra et al., 2018; Banerjee et al., 2020) and can be listed as follows:

- i) BWO without any SWS (figure 2),
- ii) Conventional BWO with rippled SWS (figure 1),
- iii) BWO with SWS replaced by 40 metamaterial-inspired identical dual ring structures (named as '40D') shown in figures 3 and 4,
- iv) BWO with SWS replaced by 40 metamaterial-inspired identical single ring structures (named as '40S') shown in figure 5,

v) BWO with SWS replaced by 20 metamaterial-inspired identical dual ring structures (named as '20D') is shown in figure 6,

vi) BWO with SWS replaced by 20 metamaterial-inspired identical single-ring structures with a central solid conductor (named '20Solid') as shown in Figures 7 and 8.

This article is arranged as follows: The Materials and Methods section presents the design and dimensional details of the six BWO configurations. The simulation results have been shown in the Results and Discussion section. Here, we discuss the effect of loading metamaterial rings inside the BWO's waveguide structure by comparing the output power, output power frequency, and efficiency results.

## Materials and Methods

### Design Consideration of BWO

The design of the BWO (Chandra et al., 2018; Banerjee et al., 2020) shown in Figure 1 is modelled using Magic3D PIC code developed by ATK Mission Systems, USA (Tan et al., 2009). Here, a SWS can be seen and it is one of the six configurations under study. The SWS is made up of five similar corrugations over a distance of 255 mm. The length of the annular cathode is 58 mm, and the thickness is 2 mm, as illustrated in Figure 1, along with all other model dimensions. In order to understand the beam wave interaction and analyze the effect of metamaterial structure, no SWS case (figure 2) was initially simulated. Later, the metamaterial BWO was analyzed by varying the number and structure of the rings. The simulation model of 40 rings of metamaterial BWO and Figure 3 and the cross-section of the same highlighting the metamaterial ring structure is shown in Figure 4. Figure 5 is the ring structure for another BWO configuration named as 40S. Figure 6 shows the placement of 20 rings of configuration 20D inside the BWO with the same ring structure as shown in Figure 4. The case of 20Solid is shown in Figures 7 and 8. Here, only a single ring structure is considered to be connected to a cylindrical central conductor inside the waveguide.

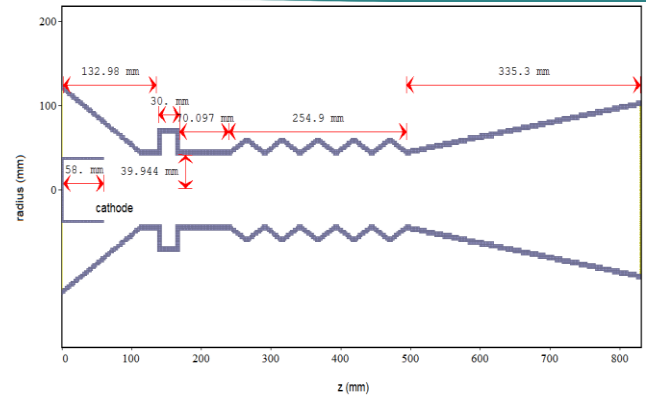


Figure 1. BWO simulation model.

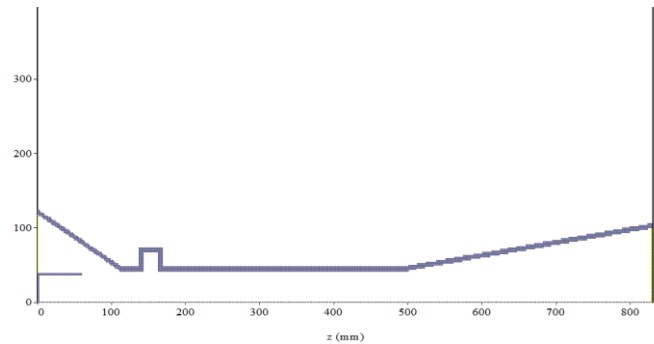


Figure 2. BWO simulation model (without SWS).

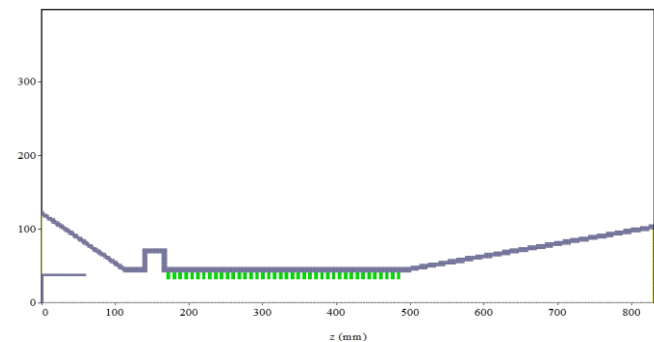


Figure 3. BWO simulation model (40D).

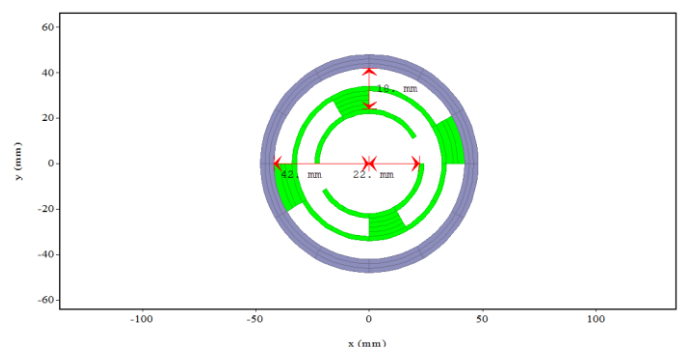


Figure 4. Ring structure for 40D BWO.

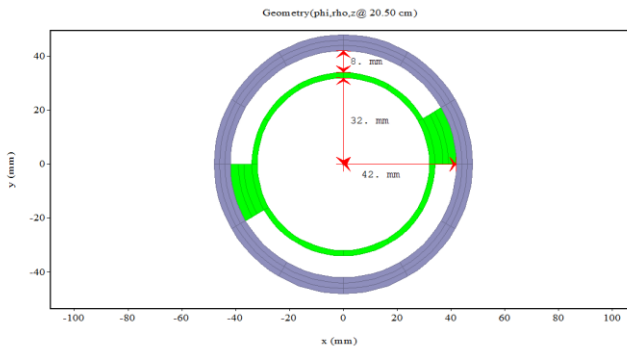


Figure 5. Ring structure for 40S BWO.

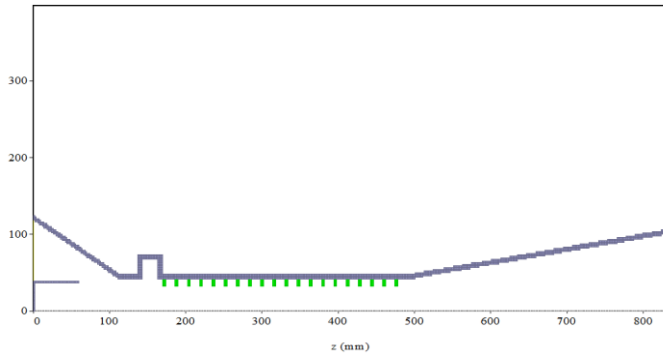


Figure 6. BWO simulation model (20D).

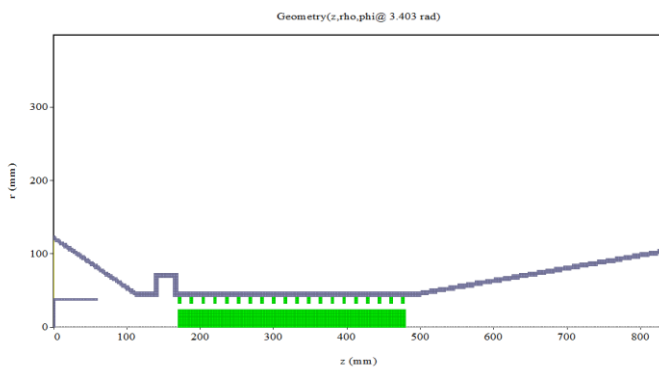


Figure 7. '20Solid' BWO configuration.

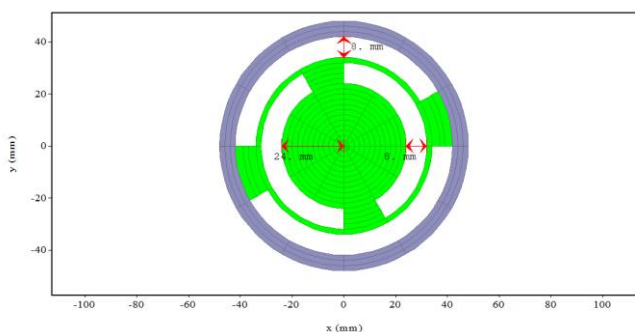


Figure 8. Ring Structure for '20Solid' BWO configuration.

**Result and Discussion**

To replicate the experimental KALI pulse, the actual device runs on a simulated high-voltage pulse

(~550V) for a short period (~100ns) (Chandra et al., 2018). The simulated magnetic field has a maximum magnitude of ~0.5T and a spatial profile represented by a fifth-order polynomial in z-coordinate. The explosive emission model simulates plasma formation on a material's surface due to electric field enhancement at micro-protrusions. The plasma typically 'emits' under the influence of the ambient electric field. The performance comparison of the six different BWO configurations is presented in Table I. The observations of different BWO configurations are summarized as follows:

i) The output obtained from the conventional rippled SWS BWO is a high power (~900MW) and high frequency (~2.7GHz) electromagnetic pulse radiated out of the device. The output microwave power is shown in figure 9 and the corresponding FFT is shown in figure 10.

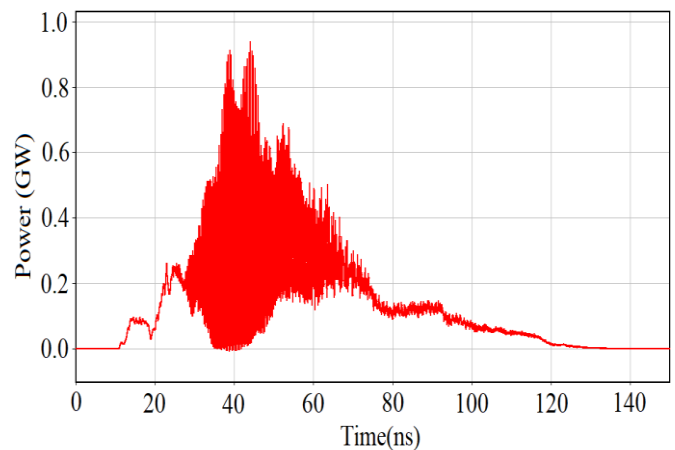


Figure 9. Simulated output power with 550kV input pulse for SWS BWO configuration

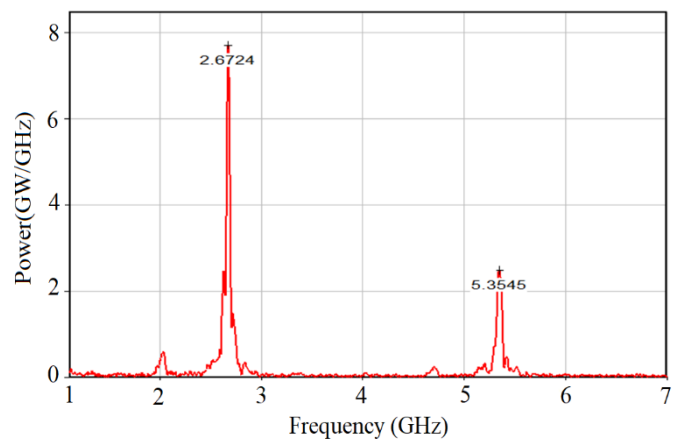


Figure 10. FFT of the output power with SWS BWO configuration.

**Table 1. Simulation Results.**

Parameters	With SWS	Without SWS	40D	40S	20D	20Solid
Input Voltage (kV)	~550	~550	~550	~550	~550	~550
Magnetic Field (T)	~0.5	~0.5	~0.5	~0.5	~0.5	~0.5
Peak Output power (GW)	~0.9	~0.55	~0.28	~0.21	~0.28	~0.6
Output Frequency (GHz)	2.67	No RF	1.35	6.62	1.329	2.6

ii) As seen in Figure 2, radio frequency is not detected when running a BWO without the appropriate SWS because when an electron beam interacts with the SWS, an electromagnetic pulse is generated.

iii) The third set of observations is obtained by replacing SWS with 40 metamaterial-inspired identical dual ring structures (named ‘40D’) as shown in figures 3 and 4, generating an electromagnetic pulse at 1.35 GHz with an output power of 280 MW.

iv) BWO, with SWS replaced by 40 metamaterial-inspired identical single-ring structures (named ‘40S’) shown in figure 5, radiates electromagnetic waves at a high frequency of around 6.62 GHz and an output power of 210 MW.

v) Figure 6 depicts the BWO with SWS replaced by 20 identical dual-ring structures inspired by metamaterials (referred to as ‘20D’). It emits electromagnetic radiation at 1.329 GHz and has an output power of 280 MW.

vi) It can be observed from figures 11 and 12 that the results of ‘20Solid’ BWO configuration are much closer to the ‘with SWS’ configuration. It has higher peak output power and efficiency than ‘40D’, ‘40S’ and ‘20D’ configurations. Also, Figure 13 shows that the output power frequency of the SWS BWO is in close agreement with ‘20Solid’ configuration. The output power and its FFT for ‘20Solid’ BWO configuration is shown in Figures 14 and 15, respectively. The peak output power generated is 0.6GW, which is closer to the generated output power due to SWS.

The data from Table I is graphically represented in Figures 11, 12 and 13, where Figure 11 represents

the peak output power, figure 12 shows the efficiency and Figure 13 shows the dominant output power frequency component for the different configurations.

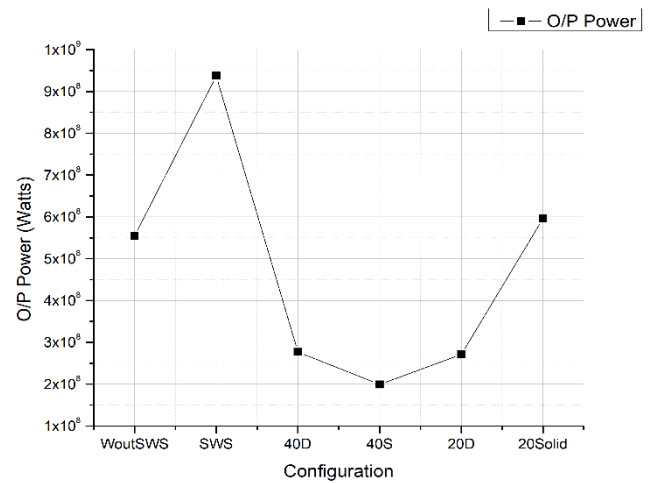


**Figure 11. Comparison of peak output power for different cases.**

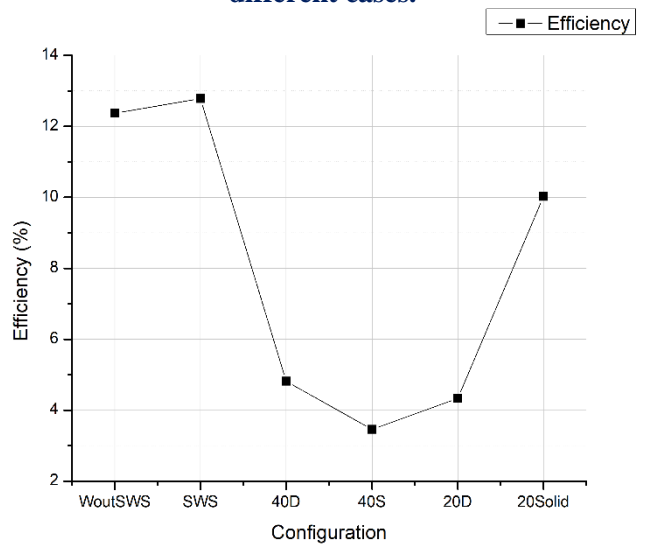


**Figure 12. Comparison of efficiency for different cases**

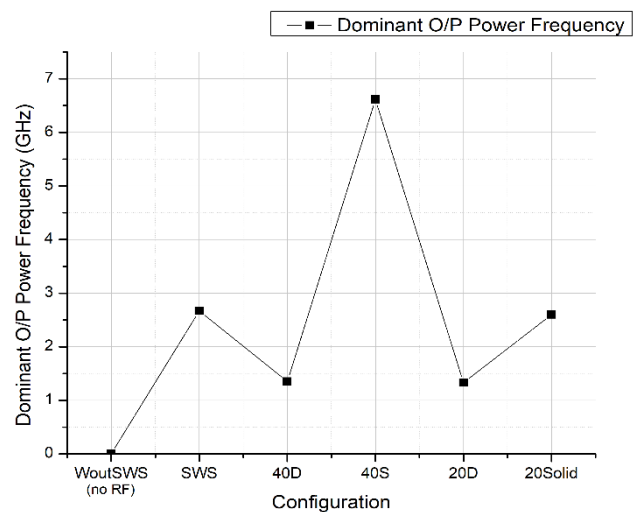


**Figure 13. Comparison of dominant output power frequency for different cases.**

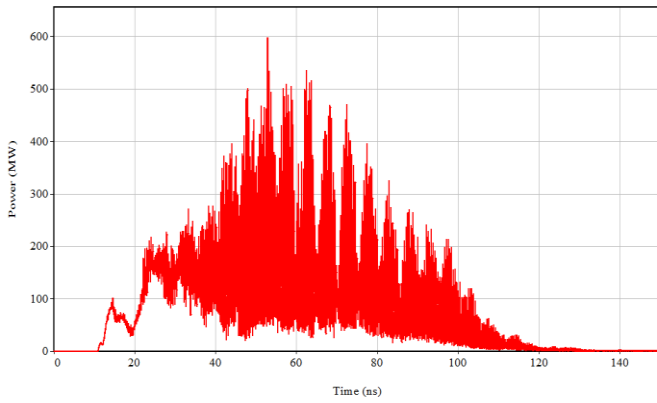


**Figure 14. Output power for '20Solid' BWO configuration.**

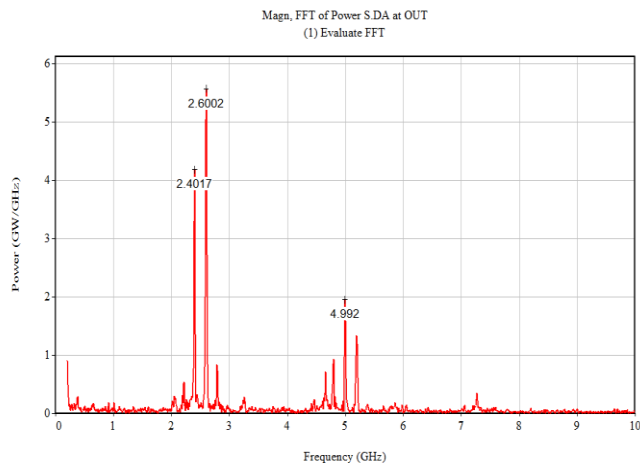


**Figure 15. Output power FFT for '20Solid' BWO configuration.**

## Conclusion

This work investigates the interactions between an annular beam cathode and several types of MTM structures in a cylindrical waveguide. We designed an axially periodic structure composed of MTM metallic plates that are replicated in the azimuthal coordinate. The study employed the Magic3D PIC code developed by ATK Mission Systems, USA (Tan et al., 2009) to obtain the necessary data for the analysis. Six different BWO configurations are simulated using the PIC code. The simulation model of an experimental device or actual BWO device has been taken as the base design for comparisons. By comparing the performance parameters of the BWO configurations, it has been found that metamaterial rings alone cannot replace or match SWS performance, but rings attached together with a solid conductor can possibly replace the SWS. However, further analysis is required regarding the optimization of the shape, material, number and design of the metamaterial rings to improve the design and performance of BWOs.

## Future scopes and limitations

However, to enhance the performance and functionality of annular beam-driven metamaterial BWOs, further mathematical modelling is needed to optimize the size, composition, quantity and configuration of the metamaterial rings.

## Conflict of interest

The authors declare no conflict of interest.

## References

- Baig, A., Diana, G., Robert, B., Calvin, D., Larry, R. B., Neville, C. L. (2012). 0.22 THz wideband sheet electron beam Traveling wave tube amplifier: Cold test measurements and beam wave interaction analysis. *Physics of Plasmas*, 19(9), 093110-1–093110-8. <https://doi.org/10.1063/1.4750048>.
- Banerjee, A. (2020). Wavelength dependent photosensitivity modulation of Aluminium/Lead sulphide/Indium tin oxide back-to-back diode. *International Int. J. Exp. Res. Rev.*, 22, 1-7. <https://doi.org/10.52756/ijerr.2020.v22.001>
- Banerjee, T. S., Ayush, S., Arti, H., Reddy, K.T.V., & Roy, A. (2020). Particle-in-cell simulation of a RBWO with experimental voltage input pulse and external magnetic field. *Physics Open*, 3, 100015. <https://doi.org/10.1016/j.physo.2020.100015>.
- Banerjee, T. S., Reddy, K. T. V., & Hadap, A. (2014). Review on microwave generation using backward wave oscillator. *Scholars Research Library, Archives of Applied Science Research*, 6(4), 129-135.
- Chandra, R., Sharma, V., Kalyanasundaram, S., Singh, S., Roy, A., Mondal, J., Mitra, S., Patel, A., Biswas, D., & Sharma, A. (2018). A Uniform, Pulsed Magnetic Field Coil for Gigawatt Operation of Relativistic Backward-Wave Oscillator. *IEEE Transactions on Plasma Science*, 46(8), 2834–2839. <https://doi.org/10.1109/TPS.2018.2850353>.
- Chen Hou-Tong, Antoinette, J. T., & Nanfang, Yu. (2016). A review of metamaterials Physics and Applications. *Reports on Progress in Physics*, 79(7), 076401. <https://doi.org/10.1088/0034-4885/79/7/076401>.

- Duan, Z., Chen, G., Jun, Z., Jucheng, L., & Min, C. (2012). Novel electromagnetic radiation in a semi-infinite space filled with a double-negative metamaterial. *Physics of Plasmas*, 19(1), 013112-1–013112-5. <https://doi.org/10.1063/1.3677888>.
- Duan, Z., Chen, G., Xin, G., & Min, C. (2013). Double negative-metamaterial based terahertz radiation excited by a sheet beam bunch. *Physics of Plasmas*, 20(9), 093301-1–093301-6. <https://doi.org/10.1063/1.4820956>.
- French, D. M., Don, S., & Keith, C. (2013). Electron beam coupling to a metamaterial structure. *Physics of Plasmas*, 20(8), 083116-1– 083116-8. <https://doi.org/10.1063/1.4817021>.
- Goplen, B., Larry, L., David, S., Gary, W. (1995). User-configurable MAGIC for electromagnetic PIC calculations. *Computer Physics Communications, Elsevier*, 87(1-2), 54-86. [https://doi.org/10.1016/0010-4655\(95\)00010-D](https://doi.org/10.1016/0010-4655(95)00010-D).
- Grow, R.W., & Watkins, D. A. (1955). Backward-Wave Oscillator Efficiency. *Proceedings of the IRE*, 43(7), 848-856. <https://doi.org/10.1109/JRPROC.1955.278151>.
- Hadap, A., Banerjee, T.S., & Saxena, A. (2020). Sheet Beam Driven Metamaterial Backward Wave Oscillator. *IEEE International Conference on Plasma Science (ICOPS)*, 978-1-7281-5307-0/20. <https://doi.org/10.1109/ICOPS37625.2020.9717696>.
- Hummelt, J.S., Samantha, M. L., Michael, A. S., & Richard, J. T. (2014). Design of Metamaterial Based Backward Wave Oscillator. *IEEE Transactions on Plasma Science*, 42(4), 930-936. <https://doi.org/10.1109/TPS.2014.2309597>.
- Jorwal, S., Dubey, A., Gupta, R., & Agarwal, S. (2023). A review: Advancement in metamaterial based RF and microwave absorbers. *Sensors and Actuators A: Physical*, 354, 114283. <https://doi.org/10.1016/j.sna.2023.114283>.
- Kumar, R., Garg, A., Shah, H., & Kaur, B. (2023). Survey on performance parameters of planar microwave antennas. *Int. J. Exp. Res. Rev.*, 31(Spl Volume), 186-194. <https://doi.org/10.52756/10.52756/ijerr.2023.v31spl.017>
- Ludeking, L., Woods, A., & Cavey, L. (2011). Magic 3.2.0 Help Manual. Alliant Techsystems (ATK), Newington, VA, USA, Technical Report.
- Marqués, R., Ferran, M., & Mario, S. (2007). *Metamaterials with Negative Parameters: Theory Design and Microwave applications*. John Wiley and Sons, ISBN: 978-0-470-19173-6.
- Mineo, M., & Claudio, P. (2010). Corrugated Rectangular Waveguide Tunable Backward Wave Oscillator for Terahertz Applications, 57(6), 1481–1484. <https://doi.org/10.1109/TED.2010.2045678>.
- Nguyen, L. B., Thomas, M. A., Gregory, S. N., Nguyen, L. B., Antonsen, T. M., & Nusinovich, G. S. (2014). Planar slow-wave structure with parasitic mode control. *IEEE Transactions on Electron Devices*, 61(6), 1600–1655. <https://doi.org/10.1109/TED.2014.2304839>.
- Pan, W., & Xiangqin, Z. (2021). Hybrid CPU- and GPU-based Implementation for Particle-in-Cell Simulation on Multicore and Multi-GPU Systems. 2021 Photonics & Electromagnetics Research Symposium (PIERS), 978-1-7281-7247-7/21, *IEEE*, pp.155-161. <https://doi.org/10.1109/PIERS53385.2021.9694911>.
- Pendry, J., B., Holden, A. J., Robbins, D. J., & Steward, W. J. (1999). Magnetism from conductors and enhanced nonlinear phenomena. *IEEE Transactions on Microwave Theory and Techniques*, 47(11), 2075-2084. <https://doi.org/10.1109/22.798002>.
- Pendry J., B., Schuring, D., & Smith, D. R. (2006). Controlling Electromagnetic Fields. *Sciences*, 312(5781), 1780-1782. <https://doi.org/10.1126/science.1125907>.
- Seidfaraji, H., Ahmed, E., Christos, C., & Edl, S. (2019). A multibeam metamaterial backward wave oscillator. *Physics of Plasmas*, 26(7), 073105-1-073105-7, <https://doi.org/10.1063/1.5100159>.
- Shapiro M. A., S. Trendafilov, Y. Urzhumov, A. Alù, R. J. Temkin, and G. Shvets (2012). Active negative-index metamaterial powered by an

- electron beam. *Physical Review B*, 86(8), 085132-1–085132-5.  
<https://doi.org/10.1103/physrevb.86.085132>.
- Shiffler, D., John, L., David, M.F., & Jack, W. (2010). A Cerenkov-like Maser Based on a Metamaterial Structure. *IEEE Transactions on Plasma Science*, 38(6), 1462-1465.  
<https://doi.org/10.1109/TPS.2010.2046914>.
- Shiffler, D., Rebecca, S., Elena, L., Erin, S., Wilkin, T., & David, F. (2013). Study of Split-Ring Resonators as a Metamaterial for High-Power Microwave Power Transmission and the Role of Defects. *IEEE Transactions on Plasma Science*, 41(6), 1679–1685.  
<https://doi.org/10.1109/TPS.2013.2251669>.
- Simovski, C.R., & Sergei, A. T. (2009) Historical Notes on Metamaterials. In: Filippo Capolino. *Theory and Phenomena of Metamaterials*. 1<sup>st</sup> edition, Taylor and Francis group, CRC Press. 10.1201/9781420054262.
- Smith, D. R., Willie, J. P., Vier, D. C., Nemat-Nasser, S. C., & Schultz, S. (2000). Composite medium with simultaneously negative permeability and permittivity. *Physical Review Letters*, 84(18), 4184-4187.  
<https://doi.org/10.1103/PhysRevLett.84.4184>.
- Tan, Y.S., & Seviour, R. (2009). Wave energy amplification in a metamaterial-based traveling-wave structure. *Europhysics Letters*, 87(3), 34005.  
<https://doi.org/10.1209/0295-5075/87/34005>.
- Tatiana, Y.A., & Andrey, V.T. (2021). Reversed Cherenkov-transition radiation in a waveguide partly filled with an anisotropic dispersive medium. *Radiation Physics and Chemistry*, 180, 109254, ISSN 0969-806X.  
<https://doi.org/10.1016/j.radphyschem.2020.109254>.
- Veselago, V. G. (1968). The electrodynamics of substances with simultaneously negative values of  $\epsilon$  and  $\mu$ . *American Institute of Physics Soviet Physics Uspekhi*, 10(4), 509-514.  
<https://doi.org/10.1070/PU1968v010n04ABEH003699>.
- Wang, Z., Yubin, G., Yanyu, W., Zhaoyun, D., Yabin, Z., Linna, Y., Huarong, G., Hairong, Y., Zhigang, L., Jin, X., & Jinjun, F. (2013). High-Power Millimeter-Wave BWO Driven by Sheet Electron Beam. *IEEE Transactions on Electron Devices*, 60(1), 471–477.  
<https://doi.org/10.1109/TED.2012.2226587>.
- Xiangyan, A., Min, C., Zheng-Ming, S., & Jie, Z. (2022). Modeling of Bound Electron Effects in Particle-in-Cell Simulation. *Communication Computational Physics*, 32(2), 583-594.  
<https://doi.org/10.4208/cicp.OA-2021-0258>.

### How to cite this Article:

Jyoti Vengurlekar and Ayush Saxena (2024). Annular Beam Driven Metamaterial Backward Wave Oscillator. *International Journal of Experimental Research and Review*, 37(Spl.), 131-138.

DOI : <https://doi.org/10.52756/ijerr.2024.v37spl.011>



This work is licensed under a Creative Commons Attribution-NonCommercial-NoDerivatives 4.0 International License.